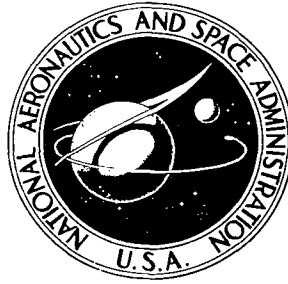


NASA TECHNICAL NOTE



NASA TN D-5302

c. 1

NASA TN D-5302



LOAN COPY: RETURN TO
AFWL (WL0L-2)
KIRTLAND AFB, N MEX

DIGITAL SIMULATION OF ROTATIONAL KINEMATICS

by Ai Chun Fang and Benjamin G. Zimmerman

Goddard Space Flight Center

Greenbelt, Md.



DIGITAL SIMULATION OF ROTATIONAL KINEMATICS

By Ai Chun Fang and Benjamin G. Zimmerman

Goddard Space Flight Center
Greenbelt, Md.

NATIONAL AERONAUTICS AND SPACE ADMINISTRATION

For sale by the Clearinghouse for Federal Scientific and Technical Information
Springfield, Virginia 22151 - Price \$3.00

ABSTRACT

This report documents a comparative study of the problems encountered in implementing the kinematic equations of rigid-body rotation. Comparing the efficiency and accuracy of the Euler angles and quaternions, the study indicates that quaternions are far superior to Euler angles for a large-angle simulation. The report explores the mechanization of the quaternion-constrained equations in order to obtain improved accuracy and simulation speed. It also describes the development of a new constraining technique (called derivative constraint) for the quaternions and stability criteria for stable solution of the constrained equations. By use of these stability criteria, the optimum feedback gain constant for the constrained kinematic equations can be selected.

CONTENTS

Abstract	ii
INTRODUCTION	1
BENCHMARK PROBLEM	2
EULER ANGLE KINEMATICS	4
FIXED-STEP INTEGRATION	5
VARIABLE-STEP INTEGRATION	5
QUATERNIONS	8
ALGEBRAIC CONSTRAINT	11
NORMALIZED CONSTRAINT	14
DERIVATIVES' CONSTRAINT	15
CONCLUSIONS	21
ACKNOWLEDGMENTS	21
References	22
Bibliography	22

DIGITAL SIMULATION OF ROTATIONAL KINEMATICS

by

Ai Chun Fang and Benjamin G. Zimmerman

Goddard Space Flight Center

INTRODUCTION

Because of the increased need for dynamic simulation of the rotational motion of rigid bodies, digital simulations have become a necessary process. To describe the angular orientation of a rigid body in such simulations, the use of both Euler angles and quaternions is very common. Therefore, it is worthwhile to make a comparative simulation study of mathematical models, using Euler angles and quaternions for the kinematic representations.

This report presents the results obtained from such a study. The report includes:

1. A discussion of Euler angles and quaternions as kinematic representations. A review of these techniques is given specifying their advantages and shortcomings.
2. An examination of integration techniques. The fourth order Runge Kutta fixed step integration technique and the variable step Runge Kutta Merson integration technique are selected for this study. Simplicity and efficiency are the primary considerations used in evaluating the relative merits of each method.
3. Presentation of significant parameters for the two representations. The following three parameters are studied in this paper:
 - (a) Simulation speed
 - (b) Attitude error (a measure of the deviation between the computed solution and the analytically determined solution)
 - (c) Constraint error (a measure of how the computed quaternion transformation matrix maintains its orthogonality)

Although the first of these parameters depends on the computing system used, a relative comparison can be made from the result presented. Double precision check runs seem to indicate that the attitude and constraint errors measured result primarily from the formulation of the model and selection of integration technique and thus are not related to the computing system.

4. Discussion of constraint error reduction techniques. In general speed and accuracy satisfy a reciprocal relationship; that is, an increase in the simulation speed means a reduction in the

accuracy. Since many simulations involve solutions extending over large time intervals, a technique for restricting error growth without reducing simulation speed is extremely desirable. Two known techniques for reducing the constraint errors are reviewed and investigated and a new technique is suggested and discussed.

5. Determination of the stability condition. The stability of the constraint error reduction technique depends upon the selection of the gain constants employed. The empirical determination of the stability conditions for a given technique and the representation of these conditions as a simple function of the system's parameters require extensive review of the computer solutions. Relationships are developed for both of the techniques for which stability is a consideration.

6. Theoretical verification for the stability conditions. The stability conditions first determined by observation of the computer solutions are then verified by the development of theoretical proofs. The conditions are thus mathematically justified for insuring stability of the computed solution and are easily implemented on a digital computer.

BENCHMARK PROBLEM

The mathematical model used in this study will be referred to as the benchmark rotational kinematics problem. The selection of the benchmark problem and the techniques used resulted from a trade-off between simplicity and applicability.

The benchmark problem, illustrated in Figure 1, consists of a fixed, right-handed orthogonal axis system $1_F, 2_F, 3_F$ and a moving axis system $1_M, 2_M, 3_M$, whose initial orientation $1_{M0}, 2_{M0}, 3_{M0}$ is obtained from $1_F, 2_F, 3_F$ by a rotation about 2_F through an angle B_o . The moving axis system moves with a constant rate ω about axis 3_F . Thus

$$\begin{aligned}\bar{2}_{M0} &= \bar{2}_F, \\ \bar{1}_F \times \bar{1}_{M0} &= (\sin B_o) \bar{2}_F, \\ \dot{\bar{1}}_M &= \omega \bar{3}_F.\end{aligned}\tag{1}$$

The actual orientation of the coordinate vectors of the moving system at time t with respect to the fixed coordinate system is

$$\begin{aligned}\bar{1}_M &= (\cos \omega t \cos B_o, \sin \omega t \cos B_o, -\sin B_o), \\ \bar{2}_M &= (-\sin \omega t, \cos \omega t, 0), \\ \bar{3}_M &= (\cos \omega t \sin B_o, \sin \omega t \sin B_o, \cos B_o).\end{aligned}\tag{2}$$

The attitude error is taken to be the maximum of the angular errors between the computed position of the coordinate axes and their actual position; that is,

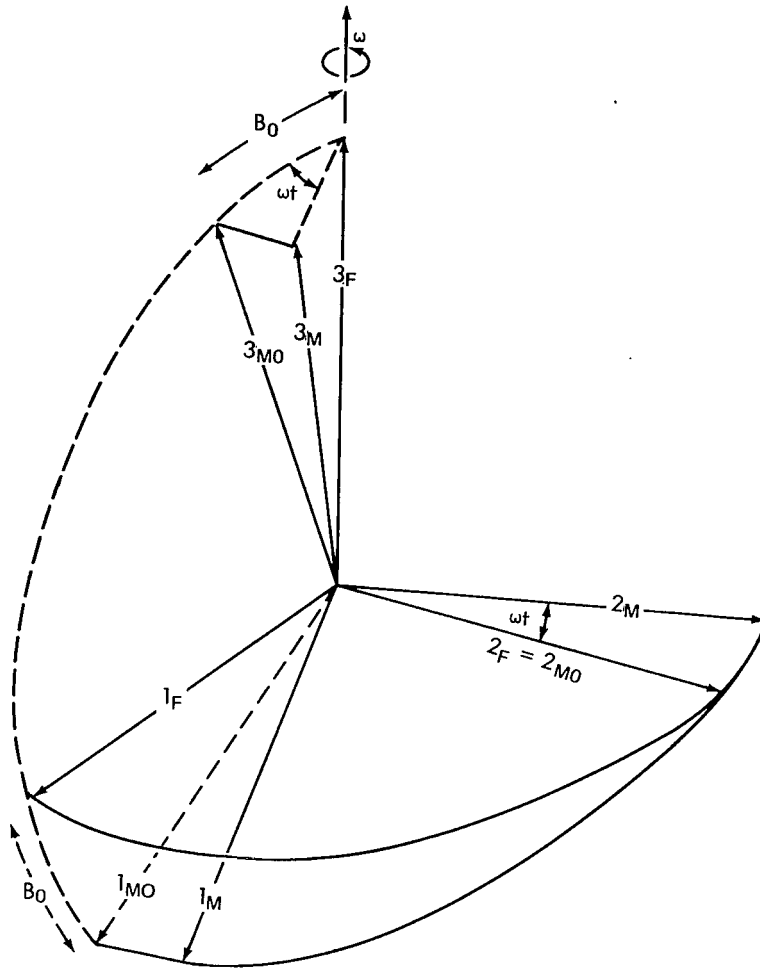


Figure 1—Coordinate systems.

$$e = \sin^{-1} \left\{ \max \left[\left| \bar{1}_M (\text{actual}) \times \bar{1}_M (\text{computed}) \right| , \right. \right. \\
 \left. \left| \bar{2}_M (\text{actual}) \times \bar{2}_M (\text{computed}) \right| , \right. \\
 \left. \left. \left| \bar{3}_M (\text{actual}) \times \bar{3}_M (\text{computed}) \right| \right] \right\} . \quad (3)$$

In determining simulation speed, the programs were rerun with the error-computing portions removed. All programs were written in FORTRAN; however, "good programming practices" were used to minimize computer time (e.g., avoidance of unnecessary subroutines, avoidance of sub-scripted variables, etc.). The simulation speed presented is calculated from solutions generated on a SDS 9300 computer.

Except where noted, the equations are considered to be normalized so that $\omega = 1$ cycle per sec. Thus both angles and the independent variable time are measured in terms of cycles (1 cycle = 2π radians). Computer time is expressed in seconds and simulation speed is determined by dividing cycles of the solution by the actual computer time required to generate it.

EULER ANGLE KINEMATICS

The use of sequences of Euler angles as kinematic parameters is quite common since they are easy to visualize and are a direct mathematical model of physical gimbal mounts. They have disadvantages in that both the kinematic differential equations and the transformation matrix involve sines and cosines of the Euler angles, the generation of which is time consuming. Also the kinematic differential equations have a singularity for certain values of the Euler angle (i.e., for those orientations for which "gimbal lock" occurs in physical gimbals). The particular Euler angle sequence selected for study is of the successive type; however, the results are general since any Euler angle sequence can be obtained from any other sequence by a suitable renumbering of the axis system, accompanied by suitable changes in the positive sense of the axes to maintain right-handedness. For Euler angles A, B, C about axes 1, 2, 3 (Figure 2) the kinematic differential equations are

$$\begin{aligned}\dot{A} &= (\cos C / \cos B) (\omega_{M_1}) - (\sin C / \cos B) (\omega_{M_2}), \\ \dot{B} &= (\sin C) (\omega_{M_1}) + (\cos C) (\omega_{M_2}), \\ \dot{C} &= -(\sin B \cos C / \cos B) (\omega_{M_1}) + (\sin B \sin C / \cos B) (\omega_{M_2}) + (\omega_{M_3}).\end{aligned}\quad (4)$$

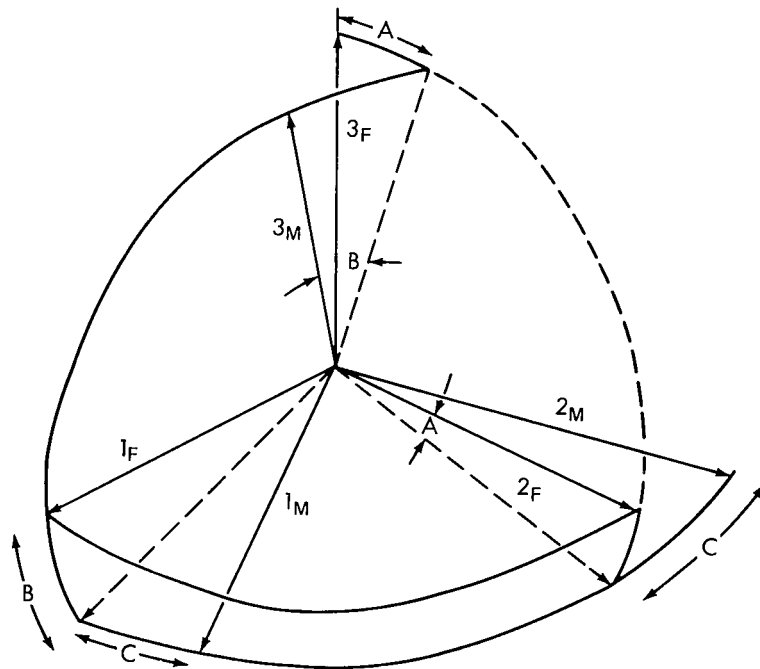


Figure 2—Euler angles.

The singularity in this system occurs when $B = \pm \pi/2$. The transformation matrix giving the moving system with respect to the fixed system is

$$\begin{bmatrix} \cos B \cos C & \sin A \sin B \cos C + \cos A \sin C & -\cos A \sin B \cos C + \sin A \sin C \\ -\cos B \sin C & -\sin A \sin B \sin C + \cos A \cos C & \cos A \sin B \sin C + \sin A \cos C \\ \sin B & -\sin A \cos B & \cos A \cos B \end{bmatrix} \quad (5)$$

Evidently, the terms of this matrix correspond to Equation 2, and thus

$$\begin{aligned} A &= \tan^{-1}(-\sin \omega t \tan B_0), \\ C &= \tan^{-1}(\tan \omega t / \cos B_0), \\ B &= \sin^{-1}(\cos \omega t \sin B_0). \end{aligned} \quad (6)$$

As ωt increases, B varies between $+B_0$ and $-B_0$. Thus the value of B_0 determines how closely the solution approaches the singular value.

FIXED-STEP INTEGRATION

Fixed-step integration techniques have the advantage of simplicity and a possible speed advantage for problems of roughly constant harmonic content. For small B_0 values, A , B , C are approximately sinusoidal, making fixed-step integration practical. When B_0 is near $\pm \pi/2$, A and C approach square waves, requiring an extremely small integration step to maintain accuracy.

Figure 3 shows attitude error, using the Runge Kutta technique versus integration step size and critical angle B_0 . This error represents the difference between a digital simulation of the benchmark problem and its true analytical solution. The estimated error per step for the integration technique is of the order of h^4 , which gives an error per cycle of the order h^3 ; the curves of constant B_0 have this form.

The selection of integration step size is accomplished best by trial and error; however, when a prior selection is required, the use of some fraction (e.g., 1/10 or less) of the period associated with the highest frequency to be encountered gives a reasonable estimate.

VARIABLE-STEP INTEGRATION

Variable-step integration techniques utilize an expression for the estimated error per step as a criterion for the dynamic adjustment of the step size. Conceptually, when the variation of the

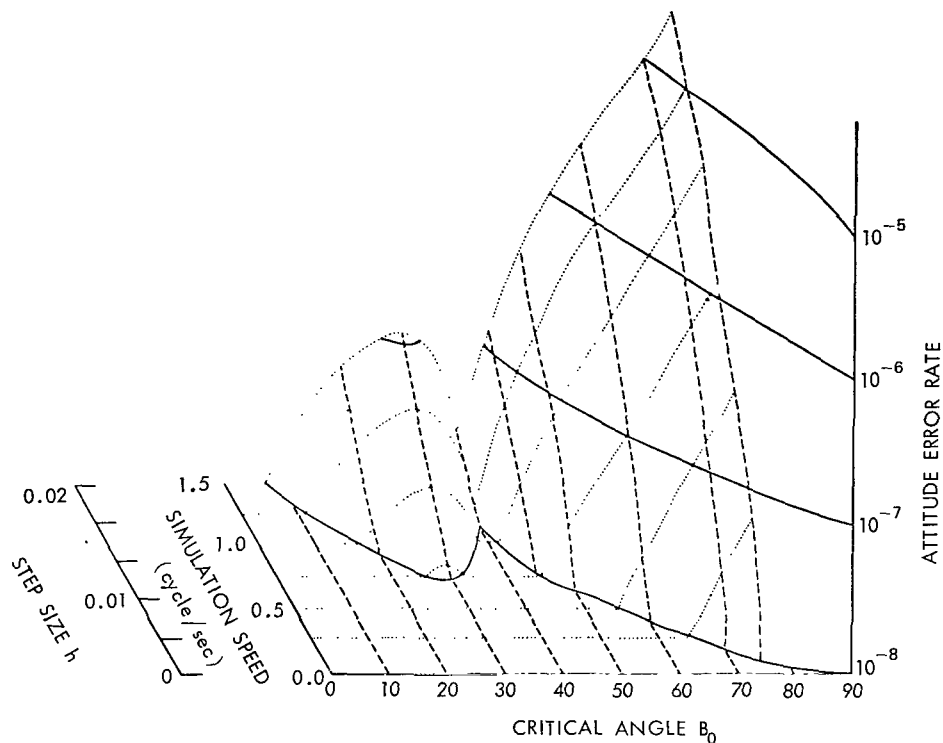


Figure 3—Euler angles with fixed-step integration.

solution is relatively smooth, the step size is increased, giving an increase in simulation speeds; when the variation of the solution increases, the step size is reduced, causing a reduction in simulation speed but tending to preserve the accuracy of the solution. The variable-step integration technique used here is the Runge Kutta Merson technique (Reference 1), which has an error per step of the order of h^4 as in the previous technique but which requires five evaluations of the derivatives per step compared to four for the previous technique. Thus, for the same step size h , the variable-step technique will take approximately 25 percent longer computing derivatives, in addition to the time required for computing and evaluating the error and adjusting the step size.

In order to adjust the step size to control the error, the following procedure is used. An estimated error for each of the state variables is computed, and the system estimated error e_s is arbitrarily taken to be the maximum of the state variable estimated errors. If e_s is greater than some preassigned value e_{max} , then the solution moves back one step and proceeds, using a step size one-half as large. If e_s is less than some preassigned value e_{min} , then the step size is doubled in succeeding steps. If $e_{min} < e_s < e_{max}$, then the solution proceeds with no change in step size. In order to keep the number of parameters to a minimum, e_{min} was set equal to e_{max} . If e_{max} is greater than e_{min} , then some increase in simulation speed can be expected; however, in no case will it be greater than 2.

Although variation of the integration error criterion can produce sizable jump discontinuities in simulation speed when using variable-step integration, if a sufficient density of solutions is obtained, the data can be smoothed so as to be presentable in a form analogous to Figure 3.

Figure 4 presents the smoothed results for the benchmark problem using the Runge Kutta Merson integration technique. Attitude error rate is plotted versus critical angle B_0 and integration speed, with the step size criterion indicated parametrically. Since the step size criterion is applied to the Euler angles rather than to the attitude error, some variation in the error criterion curves may be expected; however, they do indicate the predicted trend; i.e., as the critical angle increases, the simulation speed decreases, while the attitude error rate remains roughly constant. A comparison of Figure 3 and Figure 4 indicates that a variable integration technique has no significant advantage in simulations where the critical angle is a problem.

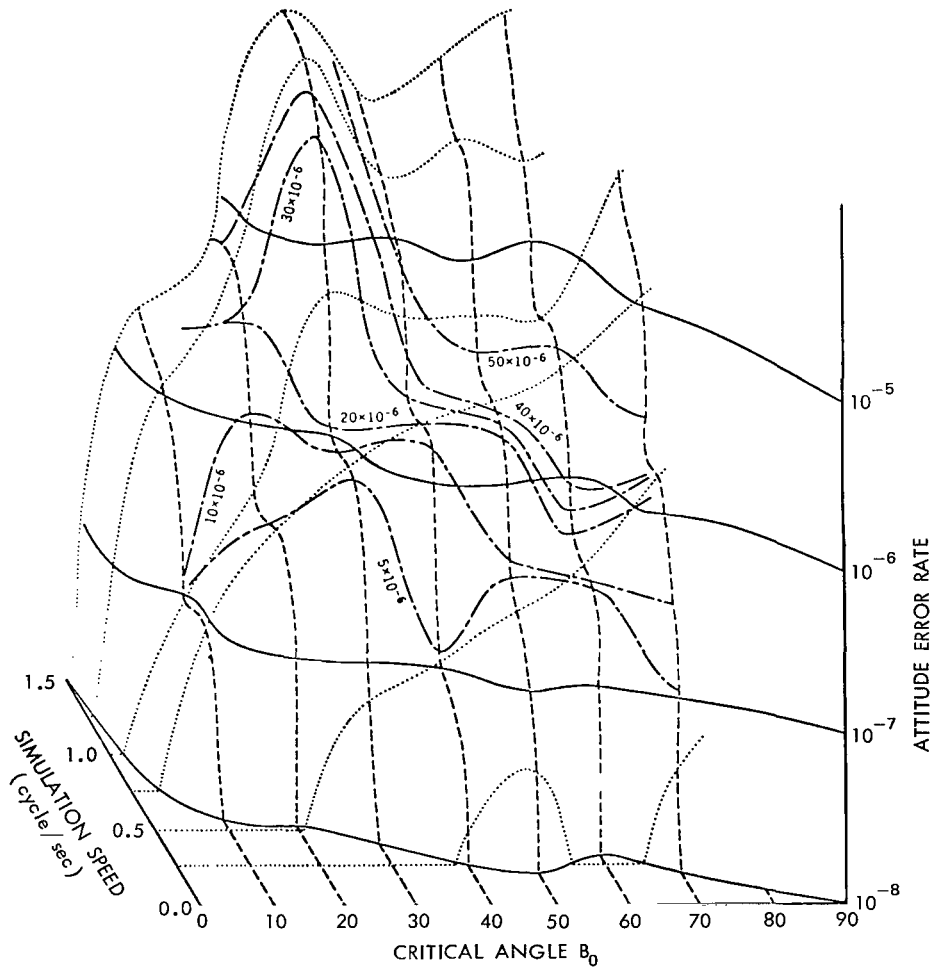


Figure 4—Euler angles with variable-step integration.

QUATERNIONS

When solving the dynamic problems associated with a rotating rigid body, the use of quaternions (or Euler's symmetric parameters) as kinematic parameters has the capacity of handling unrestricted rotation since the singularity is eliminated completely in this system. Thus the quaternions have the proven advantage of allowing simulation of a tumbling body. Also since the equations do not involve trigonometric functions, an increase in simulation speed is indicated. However, since four parameters are computed rather than the three required to describe the attitude of a body, the techniques for handling the constraint equation that relates the parameters bears consideration. For the selected benchmark problem mentioned earlier, the desired rotation is accomplished by two rotations—one through the angle B_0 about the 2_F axis, and one through the angle ωt about the axis 3_F . In quaternion notation, the first rotation, the second rotation, and the resulting rotation may be presented by q_B , q_C , and q , respectively. The quaternion q is represented

$$q = e_0 + e_1 q_1 + e_2 q_2 + e_3 q_3 , \quad (7)$$

where e_0, e_1, e_2, e_3 are real numbers regarded as the coefficient of the basis quaternions (1, q_1 , q_2 , and q_3). These basis quaternions obey the following rules of multiplication:

$$\begin{aligned} q_1^2 &= q_2^2 = q_3^2 = -1 , \\ q_1 q_2 &= -q_2 q_1 = q_3 , \\ q_2 q_3 &= -q_3 q_2 = q_1 , \\ q_3 q_1 &= -q_1 q_3 = q_2 . \end{aligned} \quad (8)$$

If the attitude of the coordinate system being described is considered as being obtained from the reference coordinate system by a single rotation, then the quaternion can be interpreted geometrically as consisting of a vector part with components e_1, e_2, e_3 having direction associated with that of the rotation axis and having magnitude equal to the sine of one-half the angle of rotation and scalar part e_0 equal to the cosine of one-half the rotation angle. Thus the quaternions q_B and q_C expressed in the fixed-coordinate system are

$$q_B = \cos B_0/2 + q_2 \sin B_0/2$$

and

$$q_C = \cos \omega t/2 + q_3 \sin \omega t/2 . \quad (9)$$

From the algebra of quaternions, q is then given by

$$\begin{aligned} q &= q_C q_B \\ &= (\cos \omega t/2 + q_3 \sin \omega t/2) (\cos B_o/2 + q_2 \sin B_o/2) . \end{aligned} \quad (10)$$

Therefore,

$$\begin{aligned} e_0 &= \cos \omega t/2 \cos B_o/2 , \\ e_1 &= - \sin \omega t/2 \sin B_o/2 , \\ e_2 &= \cos \omega t/2 \sin B_o/2 , \\ e_3 &= \sin \omega t/2 \cos B_o/2 . \end{aligned} \quad (11)$$

In terms of e_0 , e_1 , e_2 , and e_3 , Equation 2 is equivalent to

$$\begin{aligned} \bar{1}_M &= [e_0^2 + e_1^2 - e_2^2 - e_3^2, 2(e_1 e_2 + e_0 e_3), 2(e_1 e_3 - e_0 e_2)] , \\ \bar{2}_M &= [2(e_1 e_2 - e_0 e_3), e_0^2 + e_2^2 - e_1^2 - e_3^2, 2(e_2 e_3 + e_0 e_1)] , \\ \bar{3}_M &= [2(e_1 e_3 + e_0 e_2), 2(e_2 e_3 - e_0 e_1), e_0^2 + e_3^2 - e_1^2 - e_2^2] . \end{aligned} \quad (12)$$

The quaternion components are not all independent, but they satisfy the constraint equation

$$e_0^2 + e_1^2 + e_2^2 + e_3^2 = 1 . \quad (13)$$

Differentiating Equation 13 with respect to time gives

$$e_0 \dot{e}_0 + e_1 \dot{e}_1 + e_2 \dot{e}_2 + e_3 \dot{e}_3 = 0 . \quad (14)$$

The angular velocity components in the moving system can be represented as

$$\begin{aligned} (\omega_{M_1}) &= 2(e_0 \dot{e}_1 - e_1 \dot{e}_0 - e_3 \dot{e}_2 + e_2 \dot{e}_3) , \\ (\omega_{M_2}) &= 2(e_0 \dot{e}_2 - e_2 \dot{e}_0 - e_1 \dot{e}_3 + e_3 \dot{e}_1) , \\ (\omega_{M_3}) &= 2(e_0 \dot{e}_3 - e_3 \dot{e}_0 - e_2 \dot{e}_1 + e_1 \dot{e}_2) . \end{aligned} \quad (15)$$

Solving these equations and Equation 14 simultaneously yields

$$\begin{aligned}
\dot{e}_0 &= -\frac{1}{2} \left(e_1 \omega_{M_1} + e_2 \omega_{M_2} + e_3 \omega_{M_3} \right) , \\
\dot{e}_1 &= \frac{1}{2} \left(e_0 \omega_{M_1} - e_3 \omega_{M_2} + e_2 \omega_{M_3} \right) , \\
\dot{e}_2 &= \frac{1}{2} \left(e_3 \omega_{M_1} + e_0 \omega_{M_2} - e_1 \omega_{M_3} \right) , \\
\dot{e}_3 &= -\frac{1}{2} \left(e_2 \omega_{M_1} - e_1 \omega_{M_2} - e_0 \omega_{M_3} \right) .
\end{aligned} \tag{16}$$

The numerical solution of these four differential equations can be obtained without difficulty from the digital computer. A fixed-step four-point Runge Kutta integration technique was used in writing a program for this purpose. The initial values of the quaternion components at time $t(0) = 0$ are simply

$$\begin{aligned}
e_0 &= \cos (B_o/2) , \\
e_1 &= 0 , \\
e_2 &= \sin (B_o/2) , \\
e_3 &= 0 .
\end{aligned} \tag{17}$$

With any numerical integration technique, a computer gives only an approximation of the ideal solution. As noted before, machine-related errors (i.e., finite word length) and software errors (i.e., truncation of series representations of functions) are small compared with the error introduced by the integration technique. The integration step size h contributes errors that depend on the magnitude of h and tend to accumulate as the solution progresses.

For convenience, errors are divided into two types, attitude error and constraint error. The latter is defined as

$$\epsilon = 1 - \left(e_0^2 + e_1^2 + e_2^2 + e_3^2 \right) . \tag{18}$$

For the benchmark problem, both types of errors are independent of the angle B_o . They are functions of step size h only. If $h \square t - t'$ is measured in cycles, then the constraint error rate, an increment of ϵ per cycle, is expressed

$$\Delta\epsilon = \frac{(\epsilon)_t - (\epsilon)_{t'}}{h} . \tag{19}$$

The constraint error will accumulate in time to an intolerable value. In one sense, a constraint error is more serious than a position error since it represents nonorthonormality in the associated transformation matrix—a physically unrealizable situation. Reducing the constraint error by reducing h requires a correspondingly larger number of integration steps and a longer computing time. Other techniques for reducing the accumulation of constraint error are certainly needed, especially when the calculations involve direct computation of spacecraft positions over a long period of time in which a small h is impractical.

The plots of constraint error rate and attitude error rate versus h are given in Figure 5. The straight line shows the simulation time per cycle of ωt required for various values of h using the SDS 9300 computer.

Three methods of reducing the constraint error are discussed in the following paragraphs; they are algebraic constraints, normalized constraints, and derivatives constraints. These methods can improve the accuracy of solutions over the range of h for which the original system is stable.

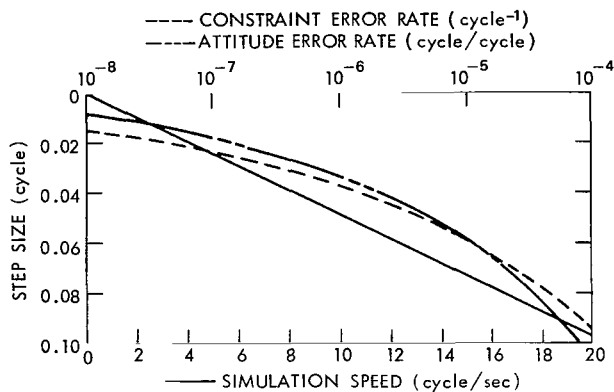


Figure 5—Quaternions with no constraint.

ALGEBRAIC CONSTRAINT

In recent years, this method has been practiced in analog simulations of spacecraft motion and has been instrumental in correcting the constraint errors (Reference 2). The method consists of adding to each equation in Equation 16 a term proportional to ϵe_0 , ϵe_1 , ϵe_2 , and ϵe_3 , respectively, giving the following constrained equations:

$$\begin{aligned}
 \dot{e}_0 &= -\frac{1}{2} \left(e_1 \omega_{M_1} + e_2 \omega_{M_2} + e_3 \omega_{M_3} \right) + K \epsilon e_0, \\
 \dot{e}_1 &= \frac{1}{2} \left(e_0 \omega_{M_1} - e_3 \omega_{M_2} + e_2 \omega_{M_3} \right) + K \epsilon e_1, \\
 \dot{e}_2 &= \frac{1}{2} \left(e_3 \omega_{M_1} + e_0 \omega_{M_2} - e_1 \omega_{M_3} \right) + K \epsilon e_2, \\
 \dot{e}_3 &= -\frac{1}{2} \left(e_2 \omega_{M_1} - e_1 \omega_{M_2} - e_0 \omega_{M_3} \right) + K \epsilon e_3.
 \end{aligned} \tag{20}$$

When Equation 20 is solved on a digital computer, the effectiveness of the technique for a given value of h requires a judicious choice for the constant K . A Liapunov function exists for the system represented by Equation 20, and, therefore, it is always stable with all $K > 0$. It can be shown that the constraint error is minimized when K is increased. However, because of quantization and

errors introduced by the integration technique, there is an upper bound of K above which Equation 20 would become unstable.

Until now, no criterion has existed for finding the maximum value of K where the constrained Equation 20 would still be stable for a given integration step size h (Reference 3). Such a criterion is derived in the following paragraphs.

The relationship between h and optimum K for the benchmark problem was first obtained empirically by repeated computer solution of Equation 20 using fixed-step Runge Kutta integration. Since this integration technique requires evaluation of the equations four times for each step, it was decided that Equation 18, required to obtain ϵ , would not be included in the integration loop, but only evaluated at the beginning of each step. It was observed from the solutions that for all

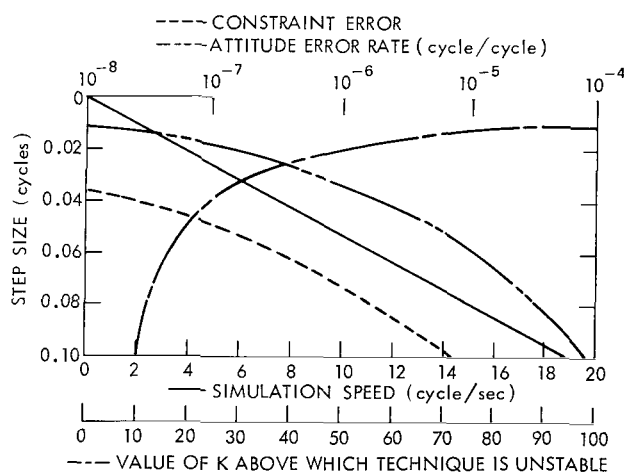


Figure 6—Quaternions with algebraic constraint.

values of $K > 0$ for which stable solutions were obtained, the constraint error did not increase with time, but assumed a constant value. As K was increased, this constant constraint error decreased, and for each h there was an optimum value K_0 of K , above which instability occurred. These results are presented in Figure 6. Comparison with Figure 5 reveals that the initial rate of increase of the attitude error is not affected by the improvement of the constraint performance. However, since the constraint error remains constant, the technique will not experience the errors introduced by nonorthonormality as would become apparent in the previously described approach as time increased.

The upper bound of K where the constrained Equation 20 remained stable was found to be

$$hK \leq 1 \quad (21)$$

Additional solutions for non-normalized values of ω revealed that the relation is independent of ω and that K_0 depends on step size h only. The important fact that K_0 is not a function of angular speed ω is quite striking. Generally speaking Equation 21 is true for any kinematic system for which quaternions are used. This result can be inferred theoretically in the following way.

If the first equation of Equation 20 is multiplied by e_0 , the second equation by e_1 , the third equation by e_2 , the fourth equation by e_3 , and these equations are summed, then the terms in the righthand side that contain ω_{M_1} , ω_{M_2} , and ω_{M_3} cancel each other. Consequently, we have

$$e_0 \dot{e}_0 + e_1 \dot{e}_1 + e_2 \dot{e}_2 + e_3 \dot{e}_3 = K \epsilon (e_0^2 + e_1^2 + e_2^2 + e_3^2) \quad (22)$$

Since

$$e_0^2 + e_1^2 + e_2^2 + e_3^2 = 1 - \epsilon \quad (23)$$

and

$$e_0 \dot{e}_0 + e_1 \dot{e}_1 + e_2 \dot{e}_2 + e_3 \dot{e}_3 = -\dot{\epsilon}/2, \quad (24)$$

Equation 22 can be written as

$$-\dot{\epsilon}/2 = K \epsilon (1 - \epsilon)$$

or

$$-\dot{\epsilon} \approx 2K\epsilon. \quad (25)$$

By using the relation

$$\dot{\epsilon} = \frac{(\epsilon)_{t+h} - (\epsilon)_t}{h} = \frac{\Delta\epsilon}{h},$$

Equation 25 becomes

$$-\Delta\epsilon \approx 2Kh\epsilon. \quad (26)$$

For a discretely sampled system to be stable, it is necessary that $|\epsilon|$ be decreasing for infinitely many integration steps; that is,

$$\left| (\epsilon)_{t+h} \right| \leq \left| (\epsilon)_t \right|,$$

which implies that $\Delta\epsilon$ is of opposite sign to ϵ and

$$|\Delta\epsilon| = \left| (\epsilon)_{t+h} - (\epsilon)_t \right| \leq \left| (\epsilon)_{t+h} \right| + \left| (\epsilon)_t \right| \leq 2 \left| (\epsilon)_t \right|. \quad (27)$$

If Equation 27 is applied to Equation 26, Equation 21 results.

This condition may require that K cannot be a very large number in some cases. For instance, if ω is small, then a large value of step size h is indicated, and the maximum permissible K will be small. Hence K does not depend on ω directly but is affected indirectly by ω through its effect on h .

NORMALIZED CONSTRAINT

When the constraint error is present, the sum of the square of the components of a quaternion

$$\left(\text{i.e., } \sum_{i=0}^3 e_i^2 \right)$$

is no longer equal to unity. The quaternion can be renormalized by dividing each of its components by this norm. This has suggested the idea that the normalization of the quaternion at each step of the integration might reduce the constraint error.

The components of the renormalized quaternion have the forms

$$\frac{e_0}{(e_0^2 + e_1^2 + e_2^2 + e_3^2)^{1/2}} \approx e_0 (1 + 1/2 \epsilon) ,$$

$$\frac{e_1}{(e_0^2 + e_1^2 + e_2^2 + e_3^2)^{1/2}} \approx e_1 (1 + 1/2 \epsilon) ,$$

$$\frac{e_2}{(e_0^2 + e_1^2 + e_2^2 + e_3^2)^{1/2}} \approx e_2 (1 + 1/2 \epsilon) ,$$

and

$$\frac{e_3}{(e_0^2 + e_1^2 + e_2^2 + e_3^2)^{1/2}} \approx e_3 (1 + 1/2 \epsilon) . \quad (28)$$

Thus $1/2 \epsilon e_0$, $1/2 \epsilon e_1$, $1/2 \epsilon e_2$, and $1/2 \epsilon e_3$ may be considered as the additional terms being added to e_0 , e_1 , e_2 , and e_3 , respectively. The derivatives are then calculated when e_0 , e_1 , e_2 , and e_3 are replaced by $e_0 + 1/2 \epsilon e_0$, $e_1 + 1/2 \epsilon e_1$, $e_2 + 1/2 \epsilon e_2$, and $e_3 + 1/2 \epsilon e_3$ in Equation 16.

Accordingly, the quaternion is normalized once every time interval h to compute the approximation of its components that are substituted and integrated in Equation 16. It is hoped that in this way the constraint error may be diminished in each interval, and the accuracy of the final solution can be improved.

The result of the computation indicated that the situation is not that simple. On one hand, the constraint error rate is less than when no constraint correction is employed, but

is not held constant as in the previous method. On the other hand, the attitude error rate (as defined previously) is not constant, but increases so that the results must be presented in terms of rate of change of attitude error rate per cycle. This higher order increase in attitude error indicates that normalization is not an effective technique for improving quaternion kinematic simulations. The results of this study are given in Figure 7.

DERIVATIVES' CONSTRAINT

At this point in the study, all the techniques for reducing the constraint error discussed in the literature have been studied. An attempt was made to develop a new technique which may serve the same purpose and be practicable also.

The most natural idea seems to be to select a function f and to approximate the equations for \dot{e} by the equations representing $(\dot{e} + f)$ for all \dot{e} 's. This function f may serve as a feedback term to force the constraint error toward zero; however, it must not disturb the stability of the system.

If each equation in Equation 16 is squared and the resulting equations added together, simplifying the results gives

$$\dot{e}_0^2 + \dot{e}_1^2 + \dot{e}_2^2 + \dot{e}_3^2 = (e_0^2 + e_1^2 + e_2^2 + e_3^2) \frac{\omega_M^2}{4}, \quad (29)$$

where

$$\omega_M^2 = \omega_{M_1}^2 + \omega_{M_2}^2 + \omega_{M_3}^2.$$

If no constraint error enters the solution, Equation 29 is simply

$$(\dot{e}_0^2 + \dot{e}_1^2 + \dot{e}_2^2 + \dot{e}_3^2) = \frac{\omega_M^2}{4}; \quad (30)$$

thus a new constraint equation has been derived based on the derivatives of the quaternions. We can define an error ϵ_d based on this constraint equation:

$$\dot{e}_0^2 + \dot{e}_1^2 + \dot{e}_2^2 + \dot{e}_3^2 = (1 - \epsilon) \frac{\omega_M^2}{4} = \frac{\omega_M^2}{4} - \epsilon_d, \quad (31)$$

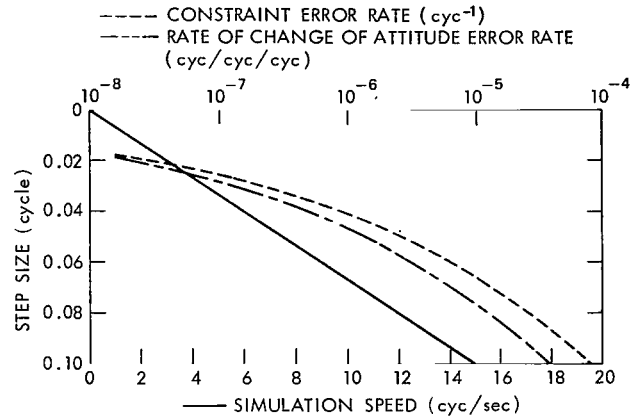


Figure 7—Quaternions with normalization.

where

$$\epsilon_d = \frac{\omega_M^2}{4} \epsilon . \quad (32)$$

It is seen that the error ϵ_d is caused by the constraint error ϵ , which affects the derivatives $\dot{\epsilon}_0$, $\dot{\epsilon}_1$, $\dot{\epsilon}_2$, and $\dot{\epsilon}_3$ directly. The function f may be chosen to take the form $\epsilon\dot{\epsilon}_0$, $\epsilon\dot{\epsilon}_1$, $\epsilon\dot{\epsilon}_2$, and $\epsilon\dot{\epsilon}_3$ for each one of the equations in Equation 16, respectively. The set of differential equations thus assumes the form

$$\begin{aligned} (\dot{\epsilon}_0)_t &= -\frac{1}{2} \left(e_1 \omega_{M_1} + e_2 \omega_{M_2} + e_3 \omega_{M_3} \right)_t + M(\epsilon)_t (\dot{\epsilon}_0)_{t-h} , \\ (\dot{\epsilon}_1)_t &= \frac{1}{2} \left(e_0 \omega_{M_1} - e_3 \omega_{M_2} + e_2 \omega_{M_3} \right)_t + M(\epsilon)_t (\dot{\epsilon}_1)_{t-h} , \\ (\dot{\epsilon}_2)_t &= \frac{1}{2} \left(e_3 \omega_{M_1} + e_0 \omega_{M_2} - e_1 \omega_{M_3} \right)_t + M(\epsilon)_t (\dot{\epsilon}_2)_{t-h} , \\ (\dot{\epsilon}_3)_t &= -\frac{1}{2} \left(e_2 \omega_{M_1} - e_1 \omega_{M_2} - e_0 \omega_{M_3} \right)_t + M(\epsilon)_t (\dot{\epsilon}_3)_{t-h} , \end{aligned} \quad (33)$$

where M is a constant. The subscript used outside the parenthesis indicates the time at which the quantity inside is being evaluated. In dealing with these equations, the constraint error, the quaternion components, and their corresponding derivatives are computed once at the end of every time interval. Their substitution into Equation 33 prepares the derivatives for the next interval.

The procedure for finding the stable value of M is similar to that used for K as described in the algebraic constraint. When ω_M and h are not normalized, then the maximum stable value of M associated with the minimum constraint error as obtained from computer solutions is, not only a function of step size, but also a function of angular speed. It was demonstrated by computer solutions that the ω_M and h associated with optimum M satisfy a reciprocal relationship; that is, the result is the same if h is multiplied by a constant, and ω_M is divided by the same constant. This is demonstrated mathematically as follows:

$$\Omega_{M_L} = \frac{\omega_{M_L}}{A} \quad L = 1, 2, 3 ,$$

and

$$\tau = Bt ,$$

where A and B are two constants. Then

$$\dot{e}_j = \frac{de_j}{dt} = \frac{de_j}{d\tau} \frac{d\tau}{dt} = B e_j' ,$$

$$j = 0, 1, 2, 3 .$$

Hence,

$$e_0' = -\frac{1}{2} \frac{A}{B} \left(e_1 \Omega_{M_1} + e_2 \Omega_{M_2} + e_3 \Omega_{M_3} \right) + M \epsilon e_0' ,$$

$$e_1' = \frac{1}{2} \frac{A}{B} \left(e_0 \Omega_{M_1} - e_3 \Omega_{M_2} + e_2 \Omega_{M_3} \right) + M \epsilon e_1' ,$$

$$e_2' = \frac{1}{2} \frac{A}{B} \left(e_3 \Omega_{M_1} + e_0 \Omega_{M_2} - e_1 \Omega_{M_3} \right) + M \epsilon e_2' ,$$

$$e_3' = -\frac{1}{2} \frac{A}{B} \left(e_2 \Omega_{M_1} - e_1 \Omega_{M_2} - e_0 \Omega_{M_3} \right) + M \epsilon e_3' . \quad (34)$$

If we set $A = B$, then the equations have the same form as the original set of equations (Equation 33); they will be satisfied by the same solution and thus have the same optimum M . However, for the original set, the step size is

$$\Delta t = h ,$$

and for the second set

$$\Delta \tau = B \Delta t = H ,$$

or

$$\Delta t = \frac{H}{B} . \quad (35)$$

Thus $H \cdot \Omega$ is equal to $h \cdot \omega$, and the product $h \cdot \omega$ can be treated as a single parameter. Next an expression was sought relating M and $h \cdot \omega$ in a simple form. As before, the practical interest centers mainly on the values of M such that the constraint error is diminished to the limit for which the system remains stable.

Extensive review of computer solutions suggested the expression

$$M \cdot (h \cdot \omega_M)^2 < 2/\pi^2$$

for $(h \cdot \omega_M)$ in cycles, or

$$M \cdot (h \cdot \omega_M)^2 < 8 \quad (36)$$

for $(h \cdot \omega_M)$ in radians.

As previously, an attempt is made to explain Equation 36 analytically. Note first that an independent stability condition $|M(\epsilon)_t| < 1$ can be established by inspection (e.g., for $\omega = 0$) from Equation 33. To establish Equation 36, the first equation of Equation 33 is multiplied by $(e_0)_t$, the second by $(e_1)_t$, the third by $(e_2)_t$, and the fourth by $(e_3)_t$. When these four equations are summed and simplified,

$$(e_0 \dot{e}_0 + e_1 \dot{e}_1 + e_2 \dot{e}_2 + e_3 \dot{e}_3)_t = M(\epsilon)_t \left[(e_0)_t (\dot{e}_0)_{t-h} + (e_1)_t (\dot{e}_1)_{t-h} + (e_2)_t (\dot{e}_2)_{t-h} + (e_3)_t (\dot{e}_3)_{t-h} \right] \cdot \quad (37)$$

That is,

$$\left(-\frac{\Delta \epsilon}{2h} \right)_t = M(\epsilon)_t \left[(e_0)_t (\dot{e}_0)_{t-h} + (e_1)_t (\dot{e}_1)_{t-h} + (e_2)_t (\dot{e}_2)_{t-h} + (e_3)_t (\dot{e}_3)_{t-h} \right] \cdot \quad (38)$$

The purpose of this technique is to constrain the derivatives such that the difference of $\omega_M^2/4$ and the sum of the square of the quaternion components' derivatives decrease. For simplicity, $(e)_t$ may be written approximately as

$$(e)_t = (e)_{t-h} + h(\dot{e})_{t-h} \cdot \quad (39)$$

Substituting Equation 39 into Equation 38 gives

$$\frac{(\Delta \epsilon)_t}{2h} = M(\epsilon)_t \left[\frac{(\Delta \epsilon)_{t-h}}{2h} - \frac{h\omega_M^2}{4} (1 - (\epsilon)_{t-h}) \right] \cdot \quad (40)$$

That is,

$$\frac{M(\epsilon)_t h^2 \omega_M^2}{2} (1 - (\epsilon)_{t-h}) = M(\epsilon)_t (\Delta \epsilon)_{t-h} - (\Delta \epsilon)_t \cdot$$

Because $(\epsilon)_t \neq 0$, and $(\epsilon)_{t-h} \ll 1$, we may write

$$\frac{M h^2 \omega_M^2}{2} \approx M(\epsilon)_t \frac{(\Delta\epsilon)_{t-h}}{(\epsilon)_t} - \frac{(\Delta\epsilon)_t}{(\epsilon)_t}, \quad (41)$$

$$\leq \left| M(\epsilon)_t \frac{(\Delta\epsilon)_{t-h}}{(\epsilon)_t} \right| + \left| \frac{(\Delta\epsilon)_t}{(\epsilon)_t} \right|. \quad (42)$$

Since $M(\epsilon)_t < 1$ for stability,

$$\frac{M h^2 \omega_M^2}{2} < \left| \frac{(\Delta\epsilon)_{t-h}}{(\epsilon)_t} \right| + \left| \frac{(\Delta\epsilon)_t}{(\epsilon)_t} \right|.$$

Near an oscillatory stability boundary,

$$(\Delta\epsilon)_{t-h} \approx -(\Delta\epsilon)_t \approx (2\epsilon)_t,$$

giving

$$\frac{M h^2 \omega_M^2}{2} < 4$$

or

$$M h^2 \omega_M^2 < 8.$$

To show that this condition includes the entire stable region, consider the value of M such that $M h^2 \omega_M^2 > 8$ and assume that at time $t-h$ the constraint error is small enough so that $|M(\epsilon)_{t-h}| < 1$. By using Equation 42, we have

$$\left| M(\epsilon)_t \frac{(\Delta\epsilon)_{t-h}}{(\epsilon)_t} \right| + \left| \frac{(\Delta\epsilon)_t}{(\epsilon)_t} \right| \geq \frac{M h^2 \omega_M^2}{2} > 4.$$

This implies that either

$$\left| \frac{(\Delta\epsilon)_t}{(\epsilon)_t} \right| > 2$$

or

$$\left| M(\epsilon)_t \frac{(\Delta\epsilon)_{t-h}}{(\epsilon)_t} \right| > 2.$$

The first of these expressions implies that after time t , $\left|(\Delta\epsilon)_t\right| > 2\left|(\epsilon)_t\right|$, and the solution is therefore unstable.

If the second inequality holds, we can write

$$\begin{aligned} M(\epsilon)_t \frac{(\Delta\epsilon)_{t-h}}{(\epsilon)_t} &= M(\epsilon)_t \left[\frac{(\epsilon)_t - (\epsilon)_{t-h}}{(\epsilon)_t} \right] \\ &= M(\epsilon)_t - M(\epsilon)_{t-h} . \end{aligned}$$

This indicates that

$$\left| M(\epsilon)_t - M(\epsilon)_{t-h} \right| > 2 ,$$

or

$$\left| M(\epsilon)_t \right| + \left| M(\epsilon)_{t-h} \right| > 2 .$$

However, it was assumed originally that

$$\left| M(\epsilon)_{t-h} \right| < 1 ;$$

thus

$$\left| M(\epsilon)_t \right| > 1 ,$$

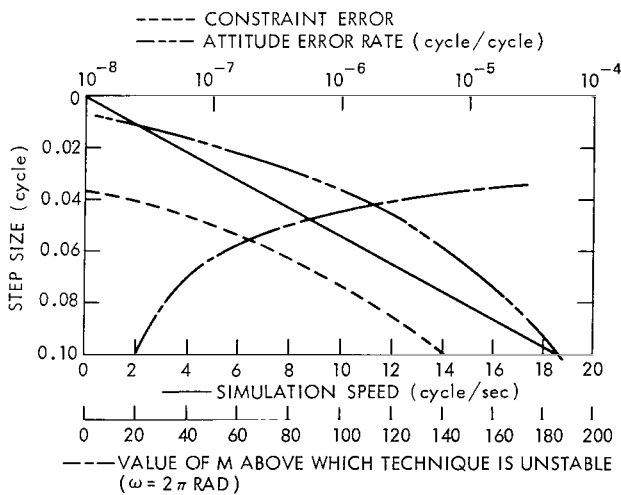


Figure 8—Quaternions with derivative constraint.

driving the solution unstable.

Since M depends on $(h\omega_M)^2$, it is natural to ask what is the stable value of M if h is held constant, but ω_M is allowed to vary. In this case, ω_M must be replaced by its maximum for the same h in Equation 36 to obtain the value of M .

Figure 8 represents the results of this technique. By comparison with the results for the algebraic constraint shown in Figure 6, it can be seen that both the attitude error rate and the constraint error are reduced.

CONCLUSIONS

This study has produced several significant results. The findings developed in the study of the benchmark problem are rather general and have application to all rotational kinematics simulations. The conclusions of this study are summarized as follows.

1. Euler angles have visual appeal, but attitude error increases as the singularity is approached.
2. The quaternion method is superior for accuracy and speed.
3. The fixed-step integration technique appears superior to the variable-step technique in simplicity and speed for simulations involving reasonable frequency variations. The relative merits for simulations involving solutions with widely varying frequency and/or amplitude can be inferred from Figures 3 and 4, but are strongly problem-related and cannot be generalized.
4. The error analyses indicate how much error may be expected in the solution for a pre-assigned step size. The results presented graphically will also assist in estimating simulation speeds.
5. In the quaternion method, the algebraic constraint technique is useful for reducing the constraint error, but it has no effect on the attitude error rate.
6. The newly proposed derivatives' constraint technique is not only as effective as the algebraic constraint technique in constraint error correction, but also diminishes the attitude error rate to a small constant value. A comparison can be made by a close examination of Figures 6 and 8.
7. The normalized constraint technique provides a small reduction in constraint error buildup, but it fails to stop the increasing of the attitude error rate. Consequently, this technique is not efficient and has less value in application.
8. The numerical stability condition for each technique has been discussed and determined. When algebraic constraint is employed, the stability condition is $h \cdot K \leq 1$, where h is the integration step size, and K is a positive constant used in implementing the constraint equation. When derivatives' constraint is used, the stability condition is $Mh^2\omega^2 < 8$, where ω is angular speed (rad/sec), and M is a positive constant used in implementing the constraint equation.

ACKNOWLEDGMENTS

The authors gratefully acknowledge the assistance of Dr. Albert J. Fleig, Jr. and Messrs. Harold P. Frisch, Peter Hui, Henry Price, and Harvey Walden in the review of this report.

Goddard Space Flight Center
National Aeronautics and Space Administration
Greenbelt, Maryland, March 7, 1969
604-31-75-02-51

REFERENCES

1. Burgin, G. H., "Midas III-A Compiler Version of Midas," *Simulation*, 6(3):160, March 1966.
2. Mitchel, E. E., and Rogers, A. E., "Quaternion Parameters in the Simulation of a Spinning Rigid Body," *Simulation*, 4(6):390, June 1965.
3. Wilson, J. W., and Steinmetz, C. G., "Analysis of Numerical Integration Techniques for Real-Time Digital Flight Simulation," NASA Technical Note D-4900, p. 63, November 1968

BIBLIOGRAPHY

- Burgin, G. H., "Midas III—A Compiler Version of Midas," *Simulation*, 6(3):160, March 1966.
- Corben, H. C., and Stehle, P., "Classical Mechanics," New York: John Wiley & Sons, Inc., p. 168, 1950.
- Frisch, H. P., "Quaternions and Their Application to the Dynamic Simulation of a Rotating Rigid Body," Goddard Space Flight Center Stabilization and Control Branch Report No. 144 (unpublished), July 1966.
- Mitchel, E. E., and Rogers, A. E., "Quaternion Parameters in the Simulation of a Spinning Rigid Body," *Simulation*, 4(6):390, June 1965.
- Mortensen, R. E., "On Systems for Automatic Control of the Rotation of a Rigid Body," University of California, Electronics Research Laboratory, Report No. 63-23, November 1963.
- Robinson, A. C., "On the Use of Quaternions in Simulation of Rigid Body Motion," WADC Technical Report 58-17, December 1958.
- Thomson, W. T., "Introduction to Space Dynamics," New York: John Wiley & Sons, Inc., p. 33, 1961.
- Whittaker, E. T., "A Treatise on the Analytical Dynamics of Particles and Rigid Bodies," Cambridge University Press, p. 8, 1960.
- Wilson, J. W., and Steinmetz, G. G., "Analysis of Numerical Integration Techniques for Real-Time Digital Flight Simulation," NASA Technical Note D-4900, p. 63, November 1968.

FIRST CLASS MAIL



POSTAGE AND FEES PAID
NATIONAL AERONAUTICS &
SPACE ADMINISTRATION

000 001 4... 01 305 69273 00903
AIR FORCE WEAPONS LABORATORY/AL117
KIRTLAND AIR FORCE BASE, NEW MEXICO 8711

UNITED STATES AIR FORCE WEAPONS LABORATORY

POSTMASTER: If Undeliverable (Section 15
Postal Manual) Do Not Return

"The aeronautical and space activities of the United States shall be conducted so as to contribute . . . to the expansion of human knowledge of phenomena in the atmosphere and space. The Administration shall provide for the widest practicable and appropriate dissemination of information concerning its activities and the results thereof."

— NATIONAL AERONAUTICS AND SPACE ACT OF 1958

NASA SCIENTIFIC AND TECHNICAL PUBLICATIONS

TECHNICAL REPORTS: Scientific and technical information considered important, complete, and a lasting contribution to existing knowledge.

TECHNICAL NOTES: Information less broad in scope but nevertheless of importance as a contribution to existing knowledge.

TECHNICAL MEMORANDUMS: Information receiving limited distribution because of preliminary data, security classification, or other reasons.

CONTRACTOR REPORTS: Scientific and technical information generated under a NASA contract or grant and considered an important contribution to existing knowledge.

TECHNICAL TRANSLATIONS: Information published in a foreign language considered to merit NASA distribution in English.

SPECIAL PUBLICATIONS: Information derived from or of value to NASA activities. Publications include conference proceedings, monographs, data compilations, handbooks, sourcebooks, and special bibliographies.

TECHNOLOGY UTILIZATION PUBLICATIONS: Information on technology used by NASA that may be of particular interest in commercial and other non-aerospace applications. Publications include Tech Briefs, Technology Utilization Reports and Notes, and Technology Surveys.

Details on the availability of these publications may be obtained from:

**SCIENTIFIC AND TECHNICAL INFORMATION DIVISION
NATIONAL AERONAUTICS AND SPACE ADMINISTRATION
Washington, D.C. 20546**